Science Advances
AAAS

advances.sciencemag.org/cgi/content/full/5/4/eaav9044/DC1

Supplementary Materials for

Hypergolic zeolitic imidazolate frameworks (ZIFs) as next-generation solid fuels: Unlocking the latent energetic behavior of ZIFs

H. M. Titi, J. M. Marrett, G. Dayaker, M. Arhangelskis, C. Mottillo, A. J. Morris,
G. P. Rachiero, T. Friščić*, R. D. Rogers*

*Corresponding author. Email: tomislav.friscic@mcgill.ca (T.F.); robin.rogers@525solutions.com (R.D.R.)

Published 5 April 2019, *Sci. Adv.* **5**, eaav9044 (2019)
DOI: 10.1126/sciadv.aav9044

The PDF file includes:

Other Supplementary Material for this manuscript includes the following:

(available at advances.sciencemag.org/cgi/content/full/5/4/eaav9044/DC1)

Data file S2. CheckCIF (in PDF format) for crystal structures of ZIF materials.
Data file S3. Movie (in MOV format) of an example drop test conducted using Co(**AIm**)$_2$, with WFNA as the oxidizer.

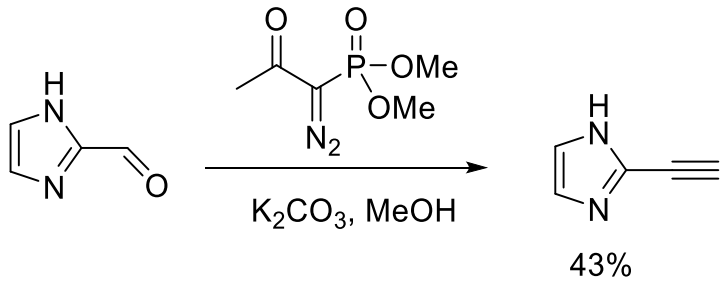

Fig. S1. Reaction scheme for the synthesis of HAIm.

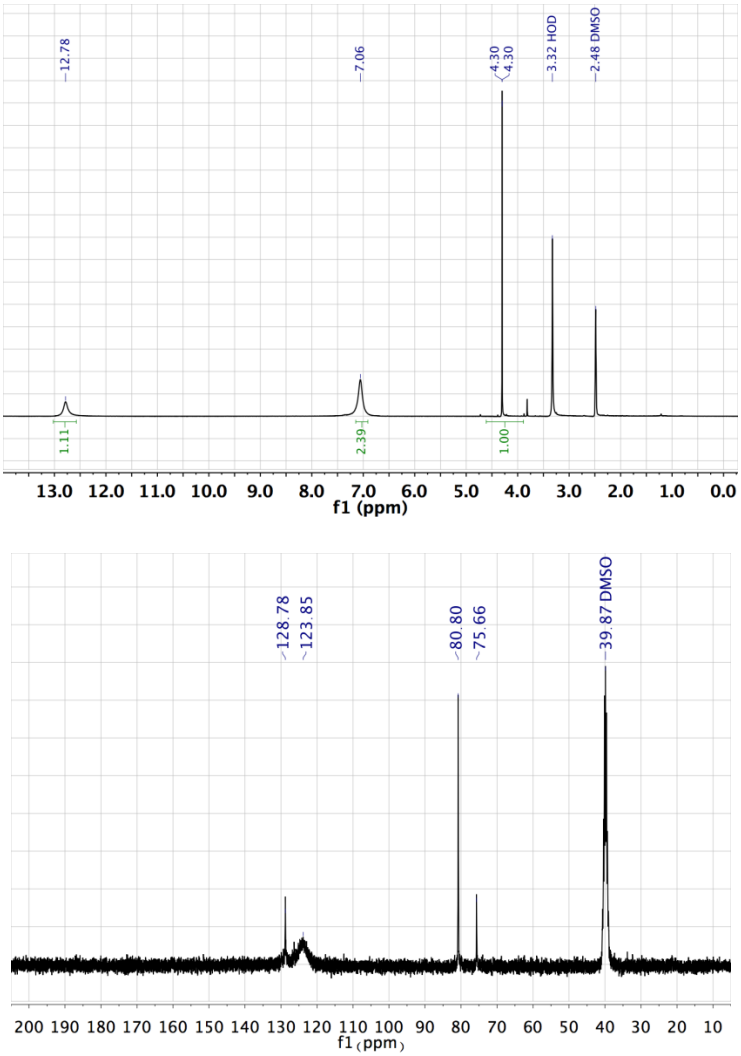

Fig. S2. NMR spectra for the ligand H**AIm**. (*top*) ^{1}H NMR spectrum and (*bottom*) ^{13}C NMR spectrum of H**AIm** recorded in DMSO-d_6.

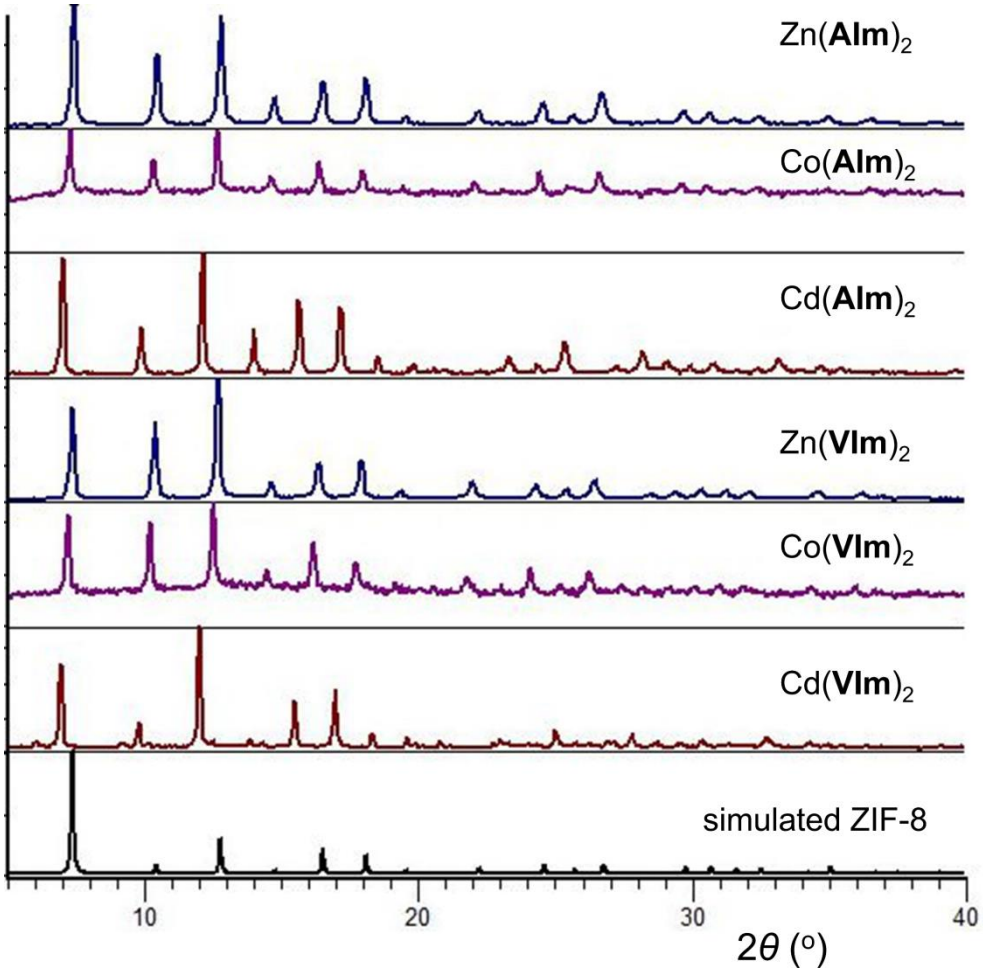

Fig. S3. Overlay of PXRD patterns of mechanochemically prepared ZIFs immediately after milling, compared to the simulated pattern for ZIF-8.

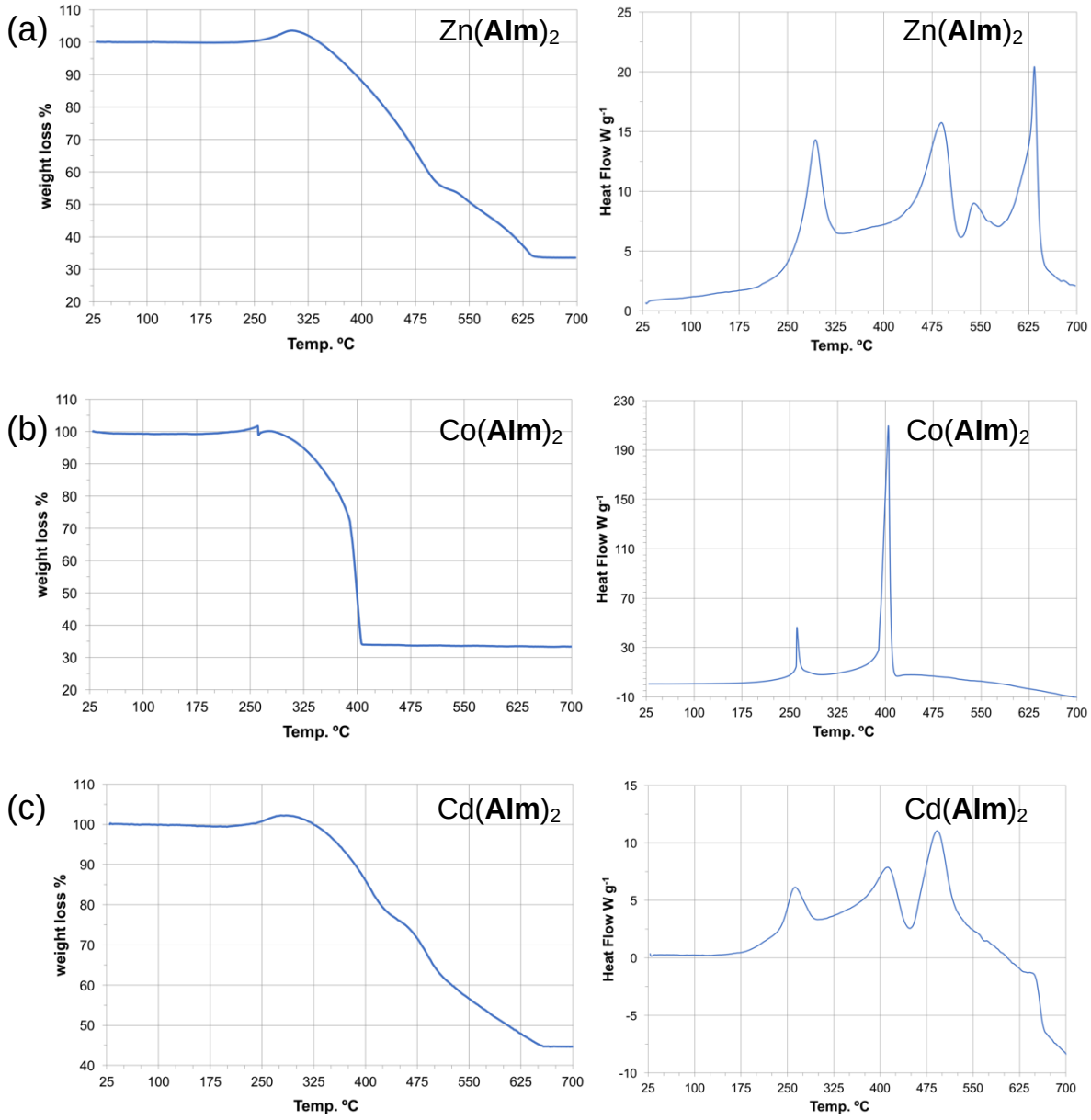

Fig. S4. Thermal analysis data for acetylene-substituted MOFs. The TGA (*left*) and DSC (*right*) thermograms of: (a) SOD-Zn(**AIm**)$_2$ in air, experimental residue: 33.6%; calculated for ZnO: 32.9%; (b) SOD-Co(**AIm**)$_2$ in air, experimental residue: 33.7%; calculated for Co_3O_4: 33.3%; (c) SOD-Cd(**AIm**)$_2$ in air, experimental residue: 44.6%; calculated for CdO: 43.5%.

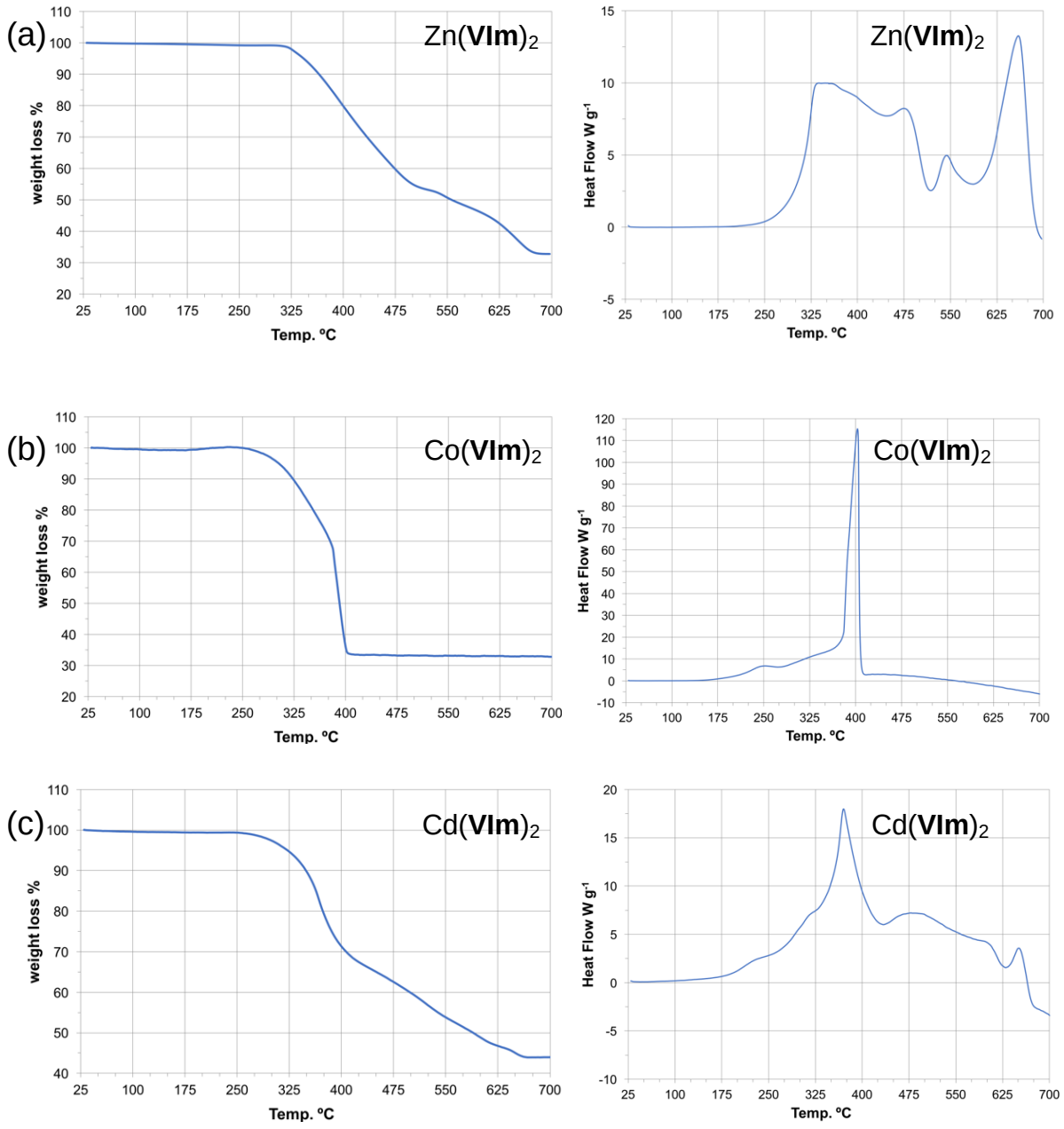

Fig. S5. Thermal analysis data for vinyl-substituted MOFs. The TGA (*left*) and DSC (*right*) thermograms recorded in air for: (a) SOD-Zn(**VIm**)$_2$, experimental residue: 33.6%; calculated for ZnO: 32.3%; (b) SOD-Co(**VIm**)$_2$, experimental residue: 33.0%; calculated for Co_3O_4: 32.7%; (c) SOD-Cd(**VIm**)$_2$, experimental residue: 43.9%; calculated for CdO: 42.9%.

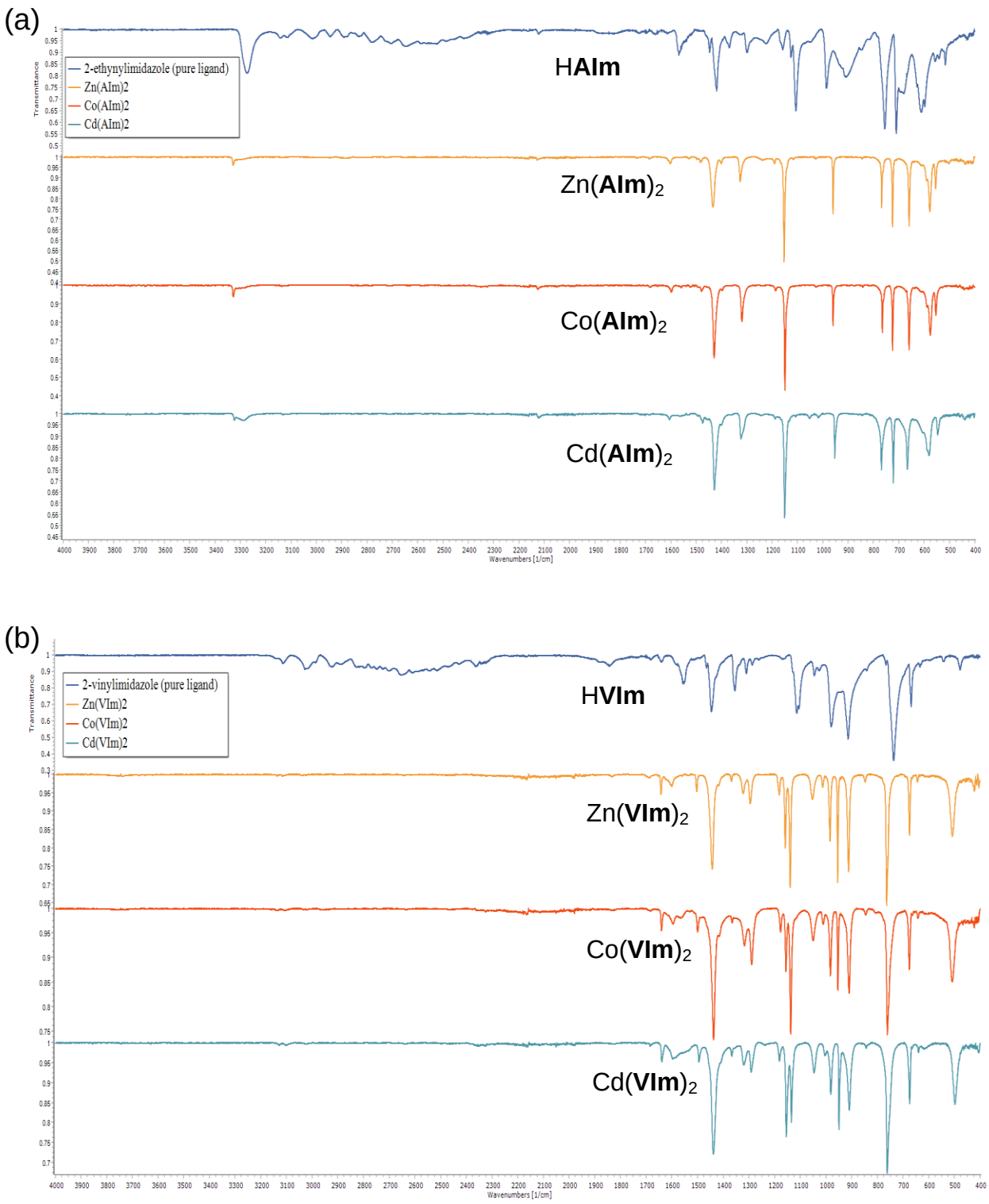

Fig. S6. Overlay of FTIR-ATR spectra for: (a) H**AIm**, Zn(**AIm**)$_2$, Co(**AIm**)$_2$, Cd(**AIm**)$_2$ and (b) H**VIm**, Zn(**VIm**)$_2$, Co(**VIm**)$_2$, Cd(**VIm**)$_2$.

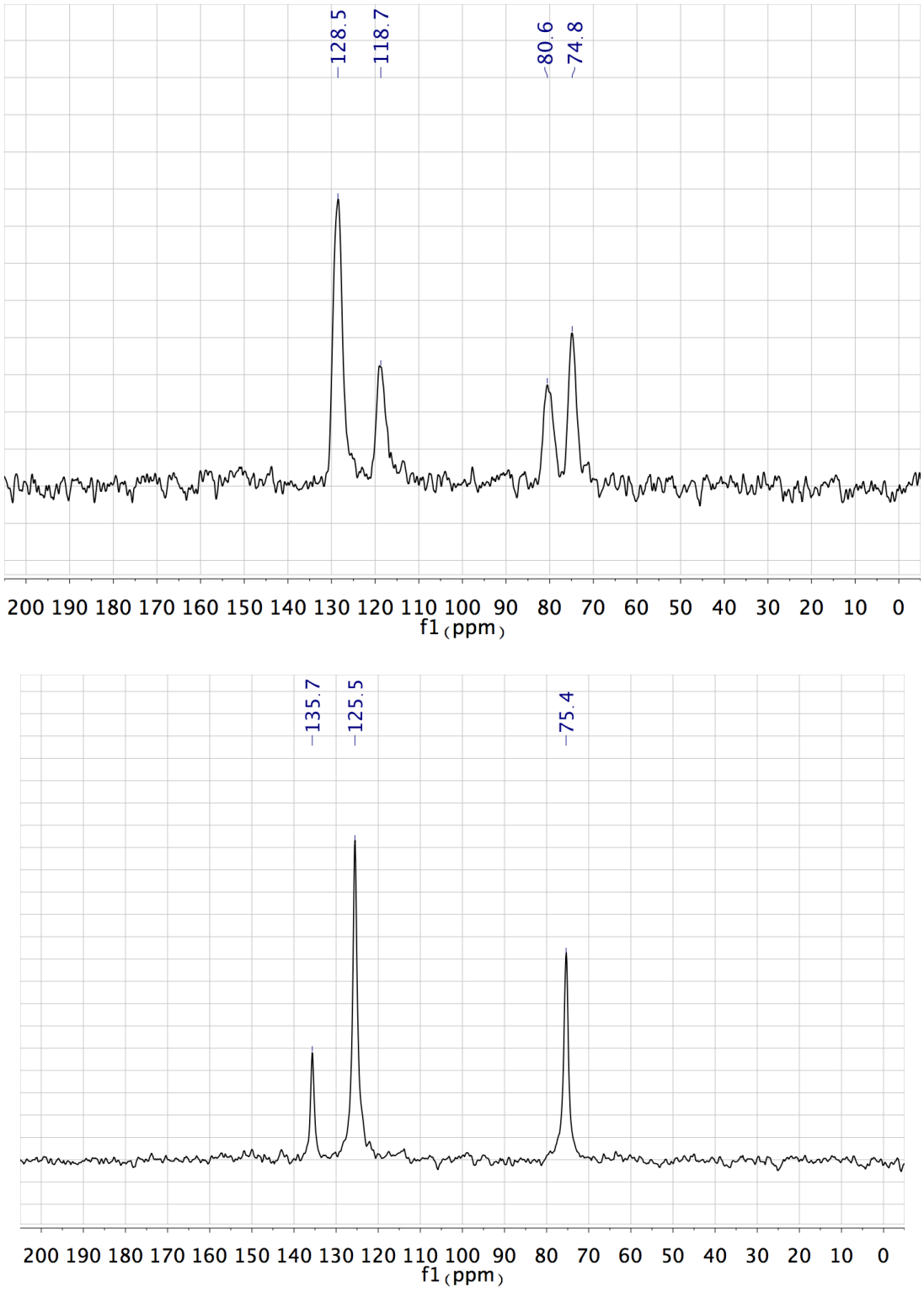

Fig. S7. Solid-state CP-MAS ^{13}C NMR spectra for: *(top)* H**AIm** and (*bottom*) SOD-Zn(**AIm**)$_2$.

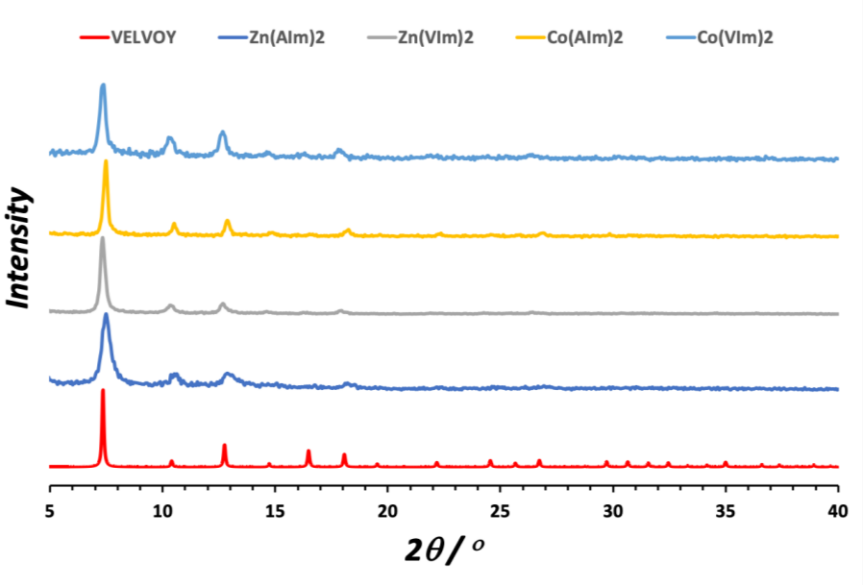

Fig. S8. Comparison of PXRD patterns for the hypergolic MOFs after 50 J impact test (from top to bottom): Zn(**AIm**)$_2$, Co(**AIm**)$_2$, Zn(**VIm**)$_2$, Co(**VIm**)$_2$ and the calculated pattern for the isostructural SOD-topology ZIF-8 (CSD code VELVOY) as a reference.

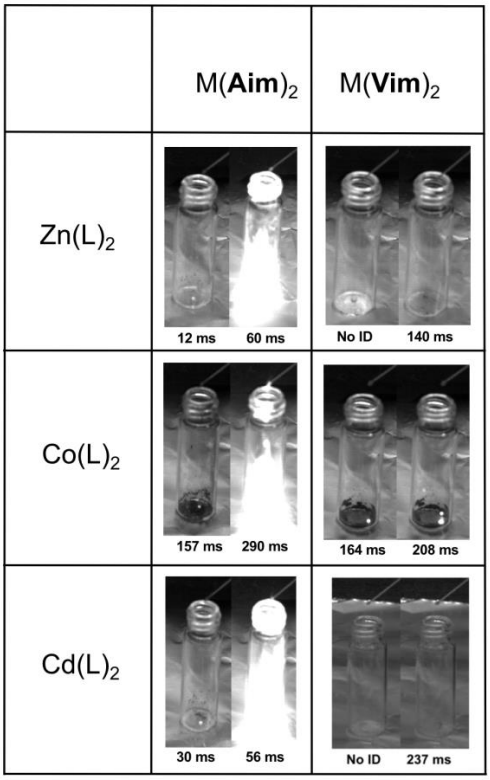

Fig. S9. Selected images of hypergolic drop tests on hypergolic ZIFs using RFNA oxidizer. In each case, the first image corresponds to the first observable frame in which ignition is visible, and the number below indicates the ID. The second image corresponds to an arbitrary point after ignition, illustrating the induced flame. Photo credit: Dr. Hatem M. Titi, McGill University.

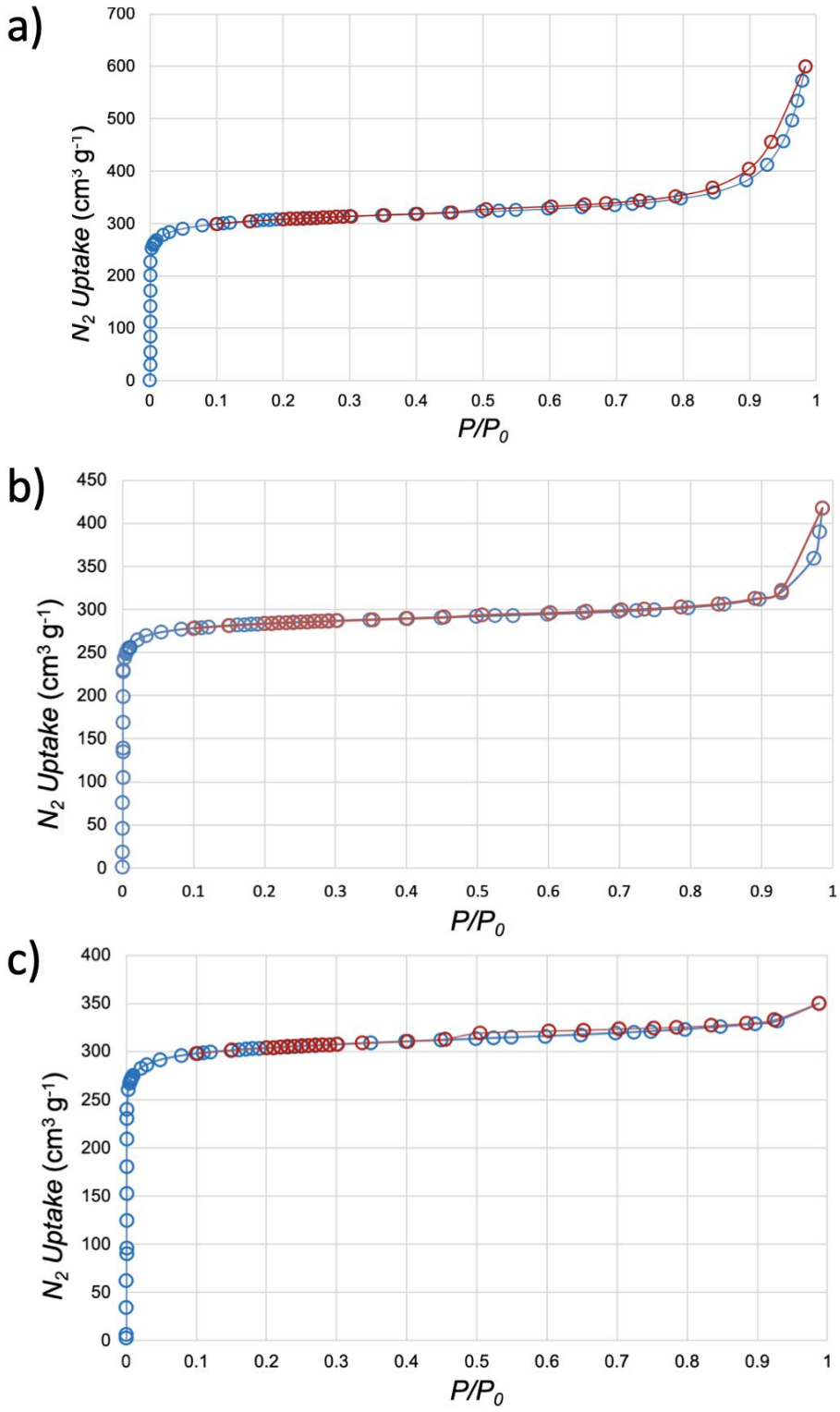

Fig. S10. Nitrogen desorption and adsorption curves for selected hypergolic MOFs after washing and evacuation: (a) Zn(**AIm**)$_2$; (b) Co(**AIm**)$_2$ and (c) Co(**VIm**)$_2$. Calculated BET surface areas for Zn(**AIm**)$_2$, Co(**AIm**)$_2$ and Co(**VIm**)$_2$ are 1215 m^2/g, 1135 m^2/g and 1210 m^2/g, respectively.

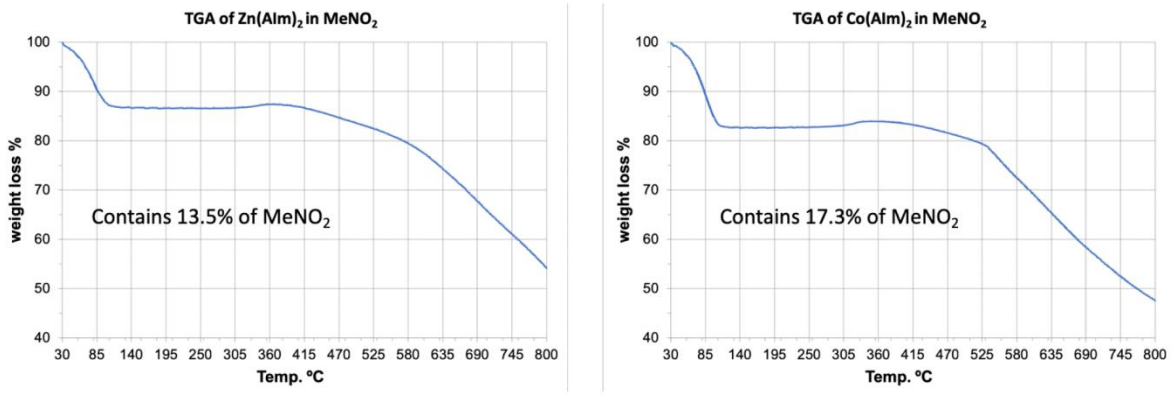

Fig. S11. Thermogravimetric analysis of (a) Zn(**AIm**)$_2$ and (b) Co(**AIm**)$_2$ after overnight suspension and stirring in nitromethane, demonstrating the inclusion of ca. 14% and 17% of nitromethane by weight.

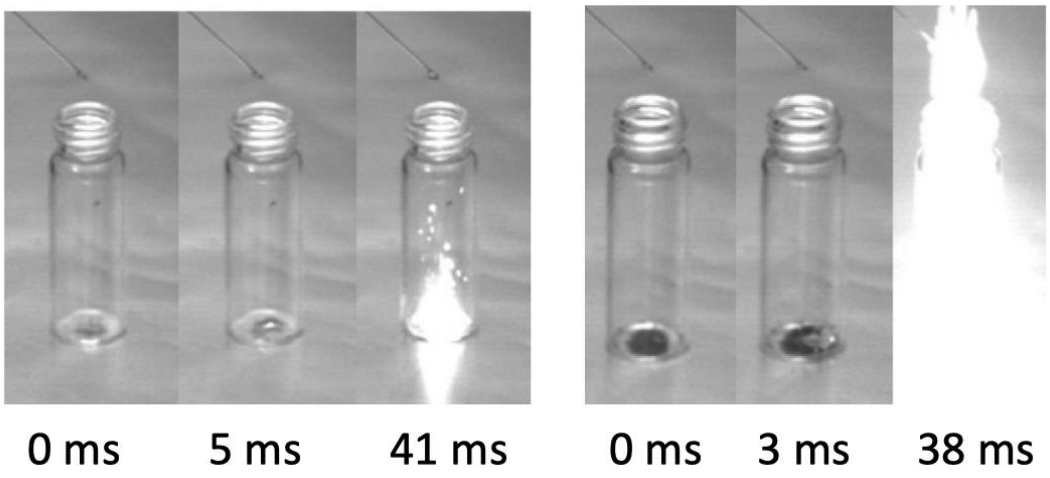

Fig. S12. Selected examples of hypergolic drop tests on ZIFs containing guests. Hypergolic drop tests for Zn(**AIm**)$_2$ (*left*) and Co(**AIm**)$_2$ (*right*) samples containing nitromethane guest. Photo credit: Dr. Hatem M. Titi, McGill University.

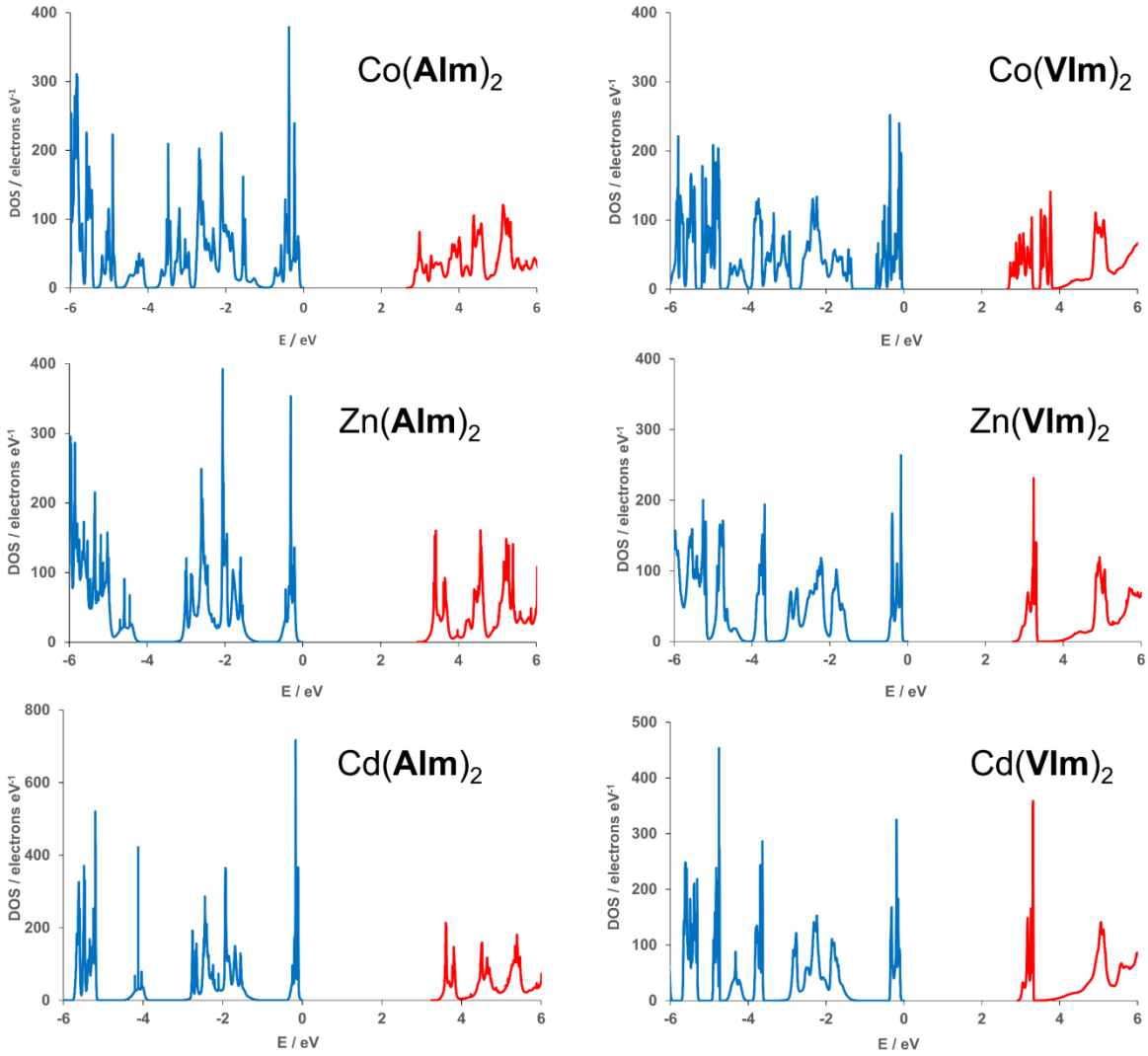

Fig. S13. Calculated DOS plots for the herein studied frameworks.

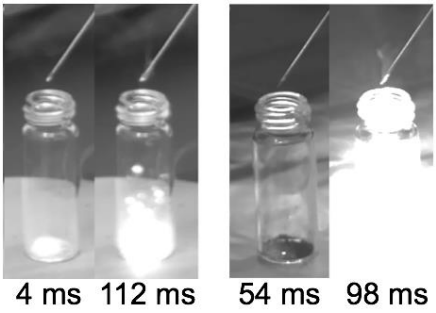

Fig. S14. The hypergolicity of selected ZIFs after 1 month using WFNA as an oxidizer. Images illustrate the behavior of: SOD-Zn(**AIm**)$_2$ (*left*) and SOD-Co(**AIm**)$_2$ (*right*). For each material, the first image corresponds to the first observable frame in which ignition is visible, and thus the number below that image is the ignition delay. The second image corresponds to an arbitrary point after ignition, and illustrates the intensity and character of the flame. Photo credit: Dr. Hatem M. Titi, McGill University.

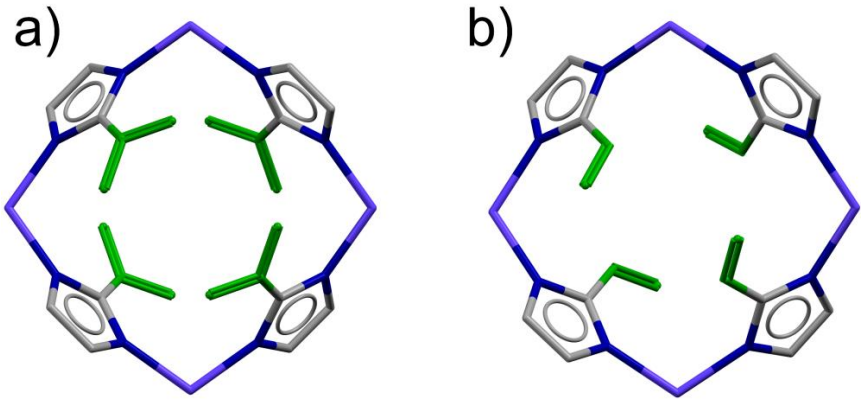

Fig. S15. Illustration of the orientation of vinyl substituents (green) in the SOD-Co(**VIm**)$_2$ structure: a) experimental structure with vinyl group disordered by mirror plane symmetry; b) ordered model missing mirror symmetry, used in periodic DFT calculations. Hydrogen atoms were omitted for clarity.

Table S1. Summary of crystallographic and Rietveld refinement parameters.

Material	Zn(**AIm**)$_2$	Co(**AIm**)$_2$	Co(V**Im**)$_2$	Cd(**AIm**)$_2$	Cd(V**Im**)$_2$
chemical formula	$Zn(C_5H_3N_2)_2$	$Co(C_5H_3N_2)_2$	$Co(C_5H_5N_2)_2$	$Cd(C_5H_3N_2)_2$	$Cd(C_5H_5N_2)_2$
M_r / g mol^{-1}	247.56	241.12	245.15	294.60	298.63
Crystal system	cubic	cubic	cubic	cubic	cubic
a / Å	17.0454(11)	16.9604(17)	17.2960(14)	17.9712(9)	18.234(2)
b / Å	17.0454(11)	16.9604(17)	17.2960(14)	17.9712(9)	18.234(2)
c / Å	17.0454(11)	16.9604(17)	17.2960(14)	17.9712(9)	18.234(2)
α / °	90	90	90	90	90
β / °	90	90	90	90	90
γ / °	90	90	90	90	90
V / Å^3	4952.5(9)	4878.8(14)	5174.1(13)	5804.0(9)	6062(2)
Space group	I -4 3 m	I -4 3 m	I -4 3 m	I -4 3 m	I -4 3 m
Density / g cm^{-3}	0.996	0.985	0.944	1.011	0.982
Radiation type	CuK_α	CuK_α	CuK_α	CuK_α	CuK_α
F(000)	1488	1452	1500	1704	1752
R_{wp}	0.118	0.048	0.065	0.068	0.076
R_p	0.092	0.036	0.050	0.055	0.058
R_{Bragg}	0.082	0.027	0.051	0.051	0.023
χ^2	4.137	1.460	2.407	1.971	3.533

Table S2. Reaction equations used in the calculation of combustion energies.

Fuel material	Reaction equation
ZIF-8	$Zn(C_4H_5N_2)_2$ (s) + 11 O_2 (g) → ZnO (s) + 8 CO_2 (g) + 2N_2 (g) + 5H_2O (g)
Zn(**VIm**)$_2$	$Zn(C_5H_5N_2)_2$ (s) + 13 O_2 (g) → ZnO (s) + 10 CO_2 (g) + 2N_2 (g) + 5H_2O (g)
Zn(**AIm**)$_2$	$Zn(C_5H_3N_2)_2$ (s) + 12 O_2 (g) → ZnO (s) + 10 CO_2 (g) + 2N_2 (g) + 3H_2O (g)
Co(**VIm**)$_2$	$Co(C_5H_5N_2)_2$ (s) + 13⅙ O_2 (g) → ⅓Co_3O_4 (s) + 10 CO_2 (g) + 2N_2 (g) + 5H_2O (g)
Co(**AIm**)$_2$	$Co(C_5H_3N_2)_2$ (s) + 12⅙ O_2 (g) → ⅓Co_3O_4 (s) + 10 CO_2 (g) + 2N_2 (g) + 3H_2O (g)
Cd(**VIm**)$_2$	$Cd(C_5H_5N_2)_2$ (s) + 13 O_2 (g) → CdO (s) + 10 CO_2 (g) + 2N_2 (g) + 5H_2O (g)
Cd(**AIm**)$_2$	$Cd(C_5H_3N_2)_2$ (s) + 12 O_2 (g) → CdO (s) + 10 CO_2 (g) + 2N_2 (g) + 3H_2O (g)

Table S3. Calculated bandgaps for herein studied ZIF structures.

Structure	**Calculated band gap / eV**
Co(**AIm**)$_2$	2.993
Zn(**AIm**)$_2$	3.475
Cd(**AIm**)$_2$	3.618
Co(**VIm**)$_2$	2.785
Zn(**VIm**)$_2$	3.070
Cd(**VIm**)$_2$	3.143

Data file S1. Crystallographic data (in CIF format) for crystal structures of ZIF materials.

Data file S2. CheckCIF (in pdf format) for crystal structures of ZIF materials.

Data file S3. Movie (in MOV format) of an example drop test conducted using Co(AIm)2, with WFNA as the oxidizer. Contact of oxidizer and the MOF is at 86 ms, and ignition takes place at 89 ms, corresponding to ID of 3 ms. The entire move length is 180 ms.